

Investigations on Laser Induced Nickel and Titanium Plasmas

M. Khaleeq-ur-Rahman, A. Latif^{*}, K.A. Bhatti, M.S. Rafique and M. K. Yousaf

Department of Physics, University of Engineering & Technology, Lahore 54890, Pakistan

Corresponding Author: Anwarlatif@uet.edu.pk

Abstract

Experiments were performed to find out plasma parameters for Nickel and Titanium metals which were irradiated in air (1 atm) to produce plasma plume using Q switched Nd: YAG pulsed laser of 1.1 MW, 10 m J, 1064 nm and 9-14 ns. Langmuir probe was used as a diagnostic tool. The signals at different probe voltages were recorded on digital storage oscilloscope. The information carried by the signals was utilized to calculate electron density, electron temperature, Debye's length and number of particles in Debye's sphere. The study shows that the calculated values of these parameters for Nickel and Titanium are different except Debye's length. Plasma parameters strongly depend on probe potentials, material used and ambient conditions.

Key Words: Nd: YAG Laser, Laser Induced Plasma, Langmuir Probe, Electron Temperature.
PACS: 52.70.-m, 52.70 Ds

1. Introduction

Laser matter interaction can produce ablation of the material especially when intense laser pulses are used. Normally it starts from desorption and may be ending at avalanche ionization. The removed mass from the target surface exhibits gas dynamics properties having moderate density, referred as laser induced plasma [1]. Several diagnostic techniques like optical emission, absorption, fluorescence and resonance ionization spectroscopy are employed for the investigation of plasma [2-6]. However, electrical diagnostic technique using Langmuir probe is significant for the study of localized behavior of plasma [7-8]. The forwardly peaked plasma plume formed as a result of ns laser pulses and metal interaction is characterized by significant plasma parameters which can be determined [9-14].

2. Experimental Setup

Nd: YAG laser (1064 nm, 10 mJ, 9 -14 ns, 1.1 MW) was used to expose the targets for the plasma production at a pressure of 1 atm. The spot sizes of the beam before and after focusing are 4mm and 12 μm respectively. The laser power density at the focus is $3 \times 10^{11} \text{ W/cm}^2$. Longmuir probe tip 2.74 cm long was inserted into the plasma. The probe was positioned 1mm from the surface of the target. Langmuir probe was biased positively as well as negatively to get electric signals recorded on 500 MHz Yokogawa

digital storage oscilloscope. The biasing circuit for the Langmuir probe is shown in Figure 1.

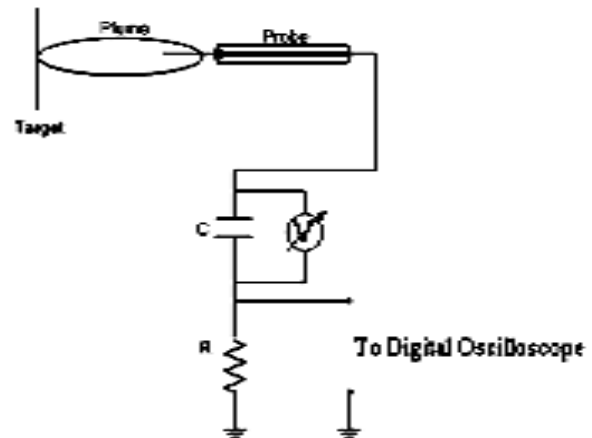


Figure 1: Biasing Circuit for Langmuir Probe

3. Results and Discussion

The signals produced by the probe as a result of targets irradiation are shown in Figure 2 and Figure 3. Langmuir probe potential was varied from +18V to -18V. Positively biased probe attracts the electrons and repels the ions from plasma plume. As a result, the sheath of electrons is developed around the probe tip. Secondary electrons produced due to air ionization can also play the role [15-18]. The negative peaks are due to the collection of ions which decrease generally with the increase in positive potential of probe.

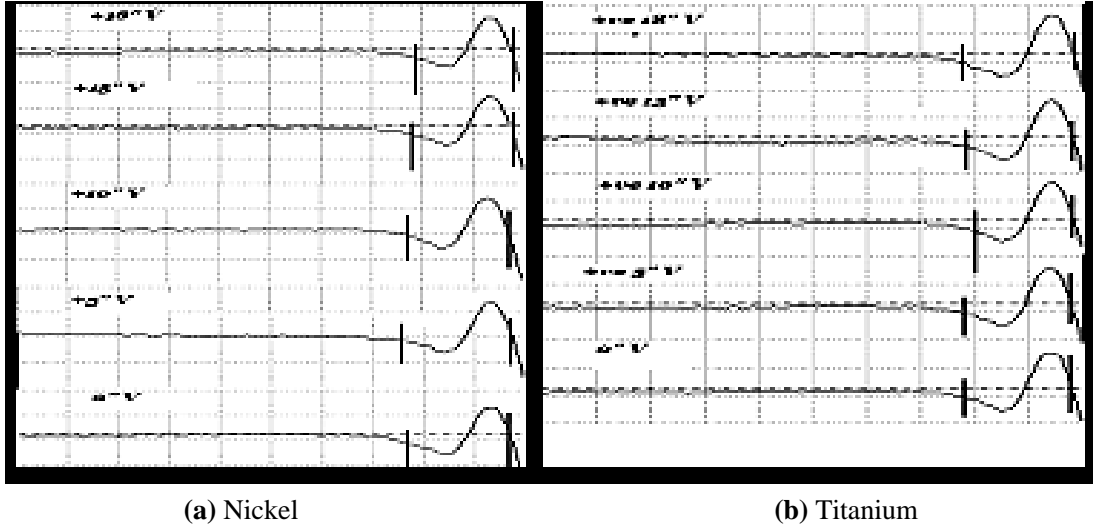


Figure 2: Langmuir Probe Signals at different Positive Potentials in Air (a) Nickel (b) Titanium (1 big square along abscissa = 20×10^{-9} s; 1 big square along ordinate = 100 mV)

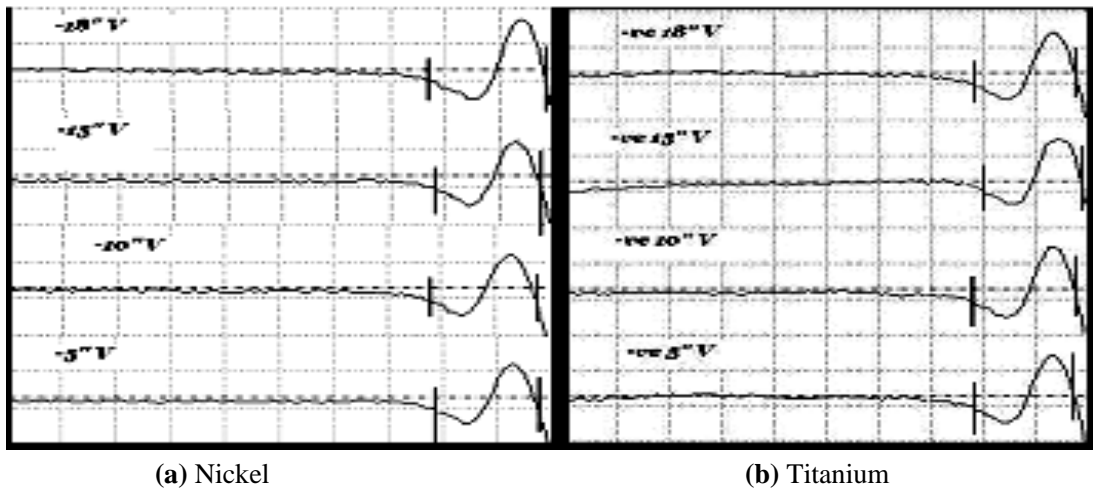


Figure 3: Langmuir Probe Signals at different negative Potentials in Air (a) Nickel (b) Titanium (1 big square along abscissa = 20×10^{-9} s; 1 big square along ordinate = 100 mV)

Table 1: Data Obtained from Langmuir probe signal in air for Nickel

Biasing Pot. V_a (Volts)	Probe Pot. V_p (Volts)	Probe Curr. I_p (Amp)	Eletron Temp. T_e (Kelvin)	Electron Density n_e (cm^{-3})	Deby's Length λ_d (m)	No. Density Deb. Sph. N_D (cm^{-3})
18	155×10^{-03}	1.4828×10^{-06}	8.0078×10^5	4.6132×10^{16}	2.8421×10^{-4}	4.4375×10^6
15	145×10^{-03}	1.3417×10^{-06}	10.7450×10^5	3.9824×10^{16}	3.5434×10^{-4}	7.2000×10^6
10	145×10^{-03}	1.3417×10^{-06}	7.1634×10^5	4.8775×10^{16}	2.6143×10^{-4}	3.6515×10^6
5	135×10^{-03}	1.2053×10^{-06}	10.3581×10^5	4.0562×10^{16}	3.4472×10^{-4}	6.9619×10^6
-5	125×10^{-03}	1.0739×10^{-06}	9.9879×10^5	4.1306×10^{16}	3.3544×10^{-4}	6.5323×10^6
-10	120×10^{-03}	1.0101×10^{-06}	9.7838×10^5	4.1735×10^{16}	3.3029×10^{-4}	6.3008×10^6
-15	120×10^{-03}	1.0101×10^{-06}	14.675×10^5	3.4076×10^{16}	4.4768×10^{-4}	12.8104×10^6
-18	150×10^{-03}	1.4117×10^{-06}	9.8402×10^5	4.1615×10^{16}	3.3172×10^{-4}	6.3647×10^6

Table2: Data Obtained from Langmuir probe signal in air for Titanium

Biassing Pot. V _a (Volts)	Probe Pot. V _p (Volts)	Probe Curr. I _p (Amp)	Eletron Temp. T _e (Kelvin)	Electron Density n _e (cm ⁻³)	Deby's Length λ _d (m)	No. Density Deb. Sph. N _D (cm ⁻³)
18	170×10 ⁻⁰³	1.7030×10 ⁻⁰⁶	15.260×10 ⁵	4.351×10 ¹⁶	4.0399×10 ⁻⁴	12.02×10 ⁶
15	165×10 ⁻⁰³	1.6280×10 ⁻⁰⁶	18.848×10 ⁵	3.915×10 ¹⁶	4.7330×10 ⁻⁴	17.392×10 ⁶
10	165×10 ⁻⁰³	1.6280×10 ⁻⁰⁶	12.565×10 ⁵	4.794×10 ¹⁶	3.4924×10 ⁻⁴	8.350×10 ⁶
5	160×10 ⁻⁰³	1.5552×10 ⁻⁰⁶	12.312×10 ⁵	4.843×10 ¹⁶	3.4390×10 ⁻⁴	8.2532×10 ⁶
-5	150×10 ⁻⁰³	1.4117×10 ⁻⁰⁶	11.945×10 ⁵	4.918×10 ¹⁶	3.3620×10 ⁻⁴	7.8302×10 ⁶
-10	145×10 ⁻⁰³	1.3417×10 ⁻⁰⁶	11.793×10 ⁵	4.960×10 ¹⁶	3.3180×10 ⁻⁴	7.5914×10 ⁶
-15	145×10 ⁻⁰³	1.3417×10 ⁻⁰⁶	17.609×10 ⁵	4.050×10 ¹⁶	4.4979×10 ⁻⁴	15.4433×10 ⁶
-18	145×10 ⁻⁰³	1.2729×10 ⁻⁰⁶	13.843×10 ⁵	4.5682×10 ¹⁶	3.755×10 ⁻⁰⁴	10.1341×10 ⁶

The increased positive potential makes electrons more capable to reach the probe tip and thus neutralizing the ions. As a consequence, these electrons will make a collision with tip of the metal causing a prominent increase in electron peak. This electronic peak will now decrease due to the transient behavior of plasma. As plasma formation is a nanosecond phenomenon, so it will decay indicating the dynamical property of plasma-boundary sheath [19]. The capacitance value of plasma sheath surrounding cylindrical probe depends on the ratio of the probe radius to sheath radius [19]. After few nanoseconds, this sheath will decrease so the ratio will decrease and as a result electronic peak decreases [20]. Time variations for plasma formation process from zero biasing potential to positive 18 potential is from 30 nanoseconds to 28 nanoseconds for Nickel target and it is from 34 nanoseconds to 30 nanoseconds for Titanium target.

Figure 3 demonstrates the signals for Nickel and Titanium plasmas for negatively biased probe. Negative peak is increasing gradually because more number of ions is collected by probe tip. The probe arrangement is such that a plasma sheath is produced around it.. Positive peak due to the collection of electrons is decreasing because now the biasing potential will push the electrons and it will act as a barrier against electrons. Only high energy electrons which are able to overcome this barrier will be collected by the probe [20].

Time variations for plasma formation process from negative 5V biasing potential to negative 18V potential is from 24 nanoseconds to 34 nanoseconds

for Nickel target and it is from 32 nanoseconds to 30 nanoseconds for Titanium target. Langmuir probe V-I characteristics curves were plotted (Figure 4) using Child Langmuir law [21].

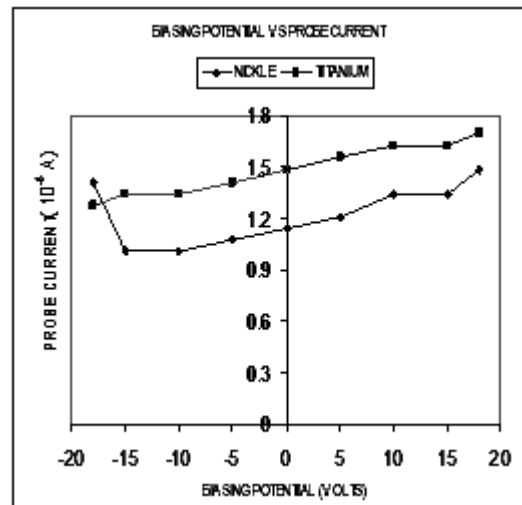


Figure 4: Potential Vs Probe Current

$$I_p = P \cdot A \cdot V^{3/2} / d^2 \tag{1}$$

Where P is a constant, called perviance, A is the area of probe tip inserted in the plasma and d is the length of probe tip inserted inside the plasma plume.

For the probe used

$$P = 2.34 \times 10^{-6},$$

$$A = 10.4 \times 10^{-6} \text{ m}^2, \quad d = 1 \times 10^{-3} \text{ m},$$

Therefore

$$I_p = 2.43 \times 10^{-5} V^{3/2} \text{ Amperes.} \tag{2}$$

Electron temperature is given by [7]

$$T_e = eV_a/k. 1/\ln(I_p/I_0)$$

Electron density of laser induced plasma can be calculated [7] by the relation given below;

$$n_e = I_0/Ae. [m_e/2\epsilon_0kT_e]^{1/2} \quad (3)$$

Debye's length of plasma is given as

$$\lambda_D = [\epsilon_0kT_e/e^2n_e]^{1/2} \quad (4)$$

Plasma frequency can be calculated as [22]

$$\omega_p = (n_e e^2 / \epsilon_0 m_e)^{1/2} \quad (5)$$

Number of particles in Debye's Sphere is given by [23]

$$N_D = n_e. 4/3. \pi \lambda_D^3. \quad (6)$$

The graphical representations of these parameters against applied probe potentials are shown in Figures 5 - 8.

The value of electron temperature was found higher in Ti than that of Ni for the same potentials. This might be due to difference in ionization energy, surface binding energy and melting point of Titanium and Nickel [8]. An exponential rise and abrupt fall is observed in electron temperature for Ni and Ti (see Figure 5). Spikes are formed when electron density was plotted against probe potentials. The electron density varies approximately at the same rate in Ni and Ti (see Figure 6). We see from equation (3), that $I_0/Ae. [m_e/2\epsilon_0K]^{1/2}$ remains constant for both Ni and Ti targets separately. Hence electron density and electron temperature are inter-dependent. Thus electron density increases gradually with increase in biasing potential for both targets as indicated in Fig.5.

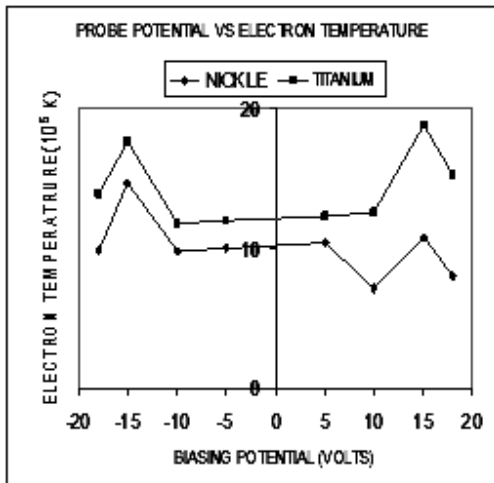


Figure 5: Potential Vs Electron Temperature

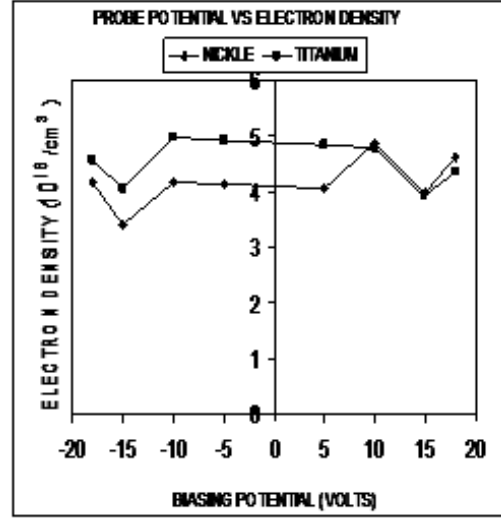


Figure 6: Potential Vs Electron Density

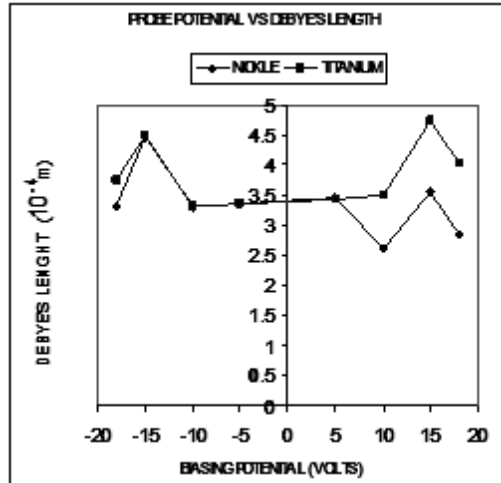


Figure 7: Potential Vs Debye Length

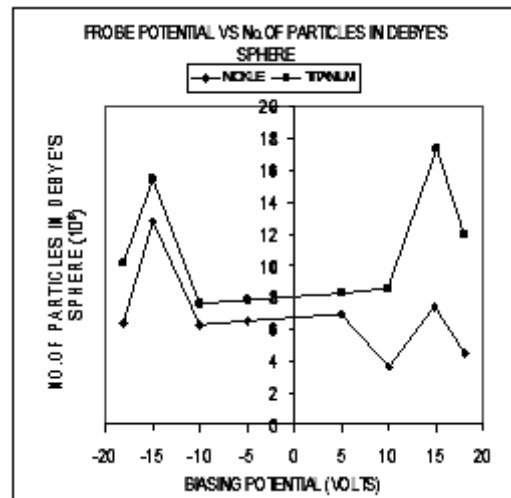


Figure 8: Potential Vs Particles in Debye's Length

Debye's lengths vary with the term $(T/n_e)^{1/2}$ only and Debye's lengths of Debye's spheres for Ni and Ti were found increasing with the increase in biasing potential of the probe due to the attraction of charged particles by the probe tip as in Figure 7. Number density of particles in Debye's sphere against the applied potentials follows the same trend as exhibited by electron temperature and Debye's length variations against the probe potentials (Figure 5 and Figure 7).

A comparative study reveals that the plasma parameters, such as, electron temperature, Debye's length, number of particles in Debye's sphere, plasma frequency etc. is different for Ni and Ti targets. The differences are due to physical properties, crystal structure, chemical properties, electron configuration and conductivity of the materials [25]. Similar work performed for other metals reveals strong dependence of these parameters on the target material and ambient environment and most of the parameters vary in different materials as a function of probe potential [25-26].

4 Conclusions

Plasma parameters are investigated with the variations in probe voltage. The negative peak of the signals obtained decreases with the increase in positive potential of probe, whereas the increase in positive peaks of the signals takes place with the increase in the biasing voltage. These peak variations caused electron temperature and electron density to change while the Debye's length remains same for both metals. The value of electron temperature was found higher in Ti than in Ni for the same potentials. All the parameters are strongly dependent on biasing potentials, target material and ambient conditions.

References

- [1] Miller, J. C. Haglund, R.F.; (1998). Laser Ablation and Desorption, Academic Press, New York.
- [2] Moenke-Blankenburg, L.; (1989). Laser Micro analysis in a series of monographs on analytic chemistry and its applications, John Wiley and Sons, New York.
- [3] Laqua, K. ; (1989). Analytical spectroscopy using laser atomizers, in analytic laser spectroscopy, Dekker, New York.
- [4] Pietsch, W. Dubreuil, B. and Briand, A.; (1995). Appl. Phys, B (61) 267.
- [5] Bidin, N. Qindeel, R. Daud, W.Y. and Bhatti, K. A. (2007). Laser Physics, (17) 1222
- [6] Harilal, S. O'Shay, S. B. and Tillack, M.S.; (2005). Journal of Applied Physics, (98) 013306.
- [7] Toftmann, B. Schou, J. Hansen, T. N. and Lunney, J. G.; (2000). Phy.Rev. Lett. (84) 3998.
- [8] Bhatti, K. A. Khaleeq-ur-Rahman, M. Rafique, Chaudhary ,K.T and Latif,A. (2010) Vacuum, (84) 980.
- [9] Rafique, M.S. Khaleeq-ur-Rahman, M. Anwar, M.S. Mahmood, F. Ashfaq, A. and Siraj, K.; (2005). Laser and Particle Beams, (23) 131.
- [10] Batani, D. Alba, S. Lombardi, P. and Galassi, A.; (1997). Rev. of Sci. Inst., 68(11) 4043.
- [11] Brandt, C. Testrich, H. R. Kozakov. and Wilke, C.; (2006). Rev. Sci. Instrum, (77) 023504
- [12] Lunt, T. Calderon, E. Fussmann, G and Hidalgo, C. (2005). Proc. conference on plasma physics, 1.005.
- [13] Noguchi, M.. Hirao, T. Shindo, M. Takemoto, Y. Kitachi, N and Namba, K.; (2003). Sou. Sci. Tech (12) 403.
- [14] Rousseau, A. Tebou, E. and Lang, N.; (2002). Appl. Phys, (92) 346.
- [15] Constantin, C. Back, C. A. Fournier, K.B.:(2005). Phys. Plasmas, (12) 063104.
- [16] Back, C. A. Grun, J. Dewald, E.L.; (2003). Plasmas Phys, (10) 2047 .
- [17] Fournier, K.B. Constantin, C. Poco J. Miller, M. C. Suter, L. J. Satcher, J. Davis, J and Grun, J.; (2004) Phys. Rev. Lett, (92) 165005.

- [18] Hendron, J. M. Mahony, C. M and Morrow, T.; (1997). *J. Appl. Phys.* (81) 2131.
- [19] Heidecker, E. Schafer, J. H. and Busch, U. J. ;(1988) *J. Appl. Phys.* (64) 2291.
- [20] Weaver, I. Martin, G.W. and Graham W.; (1999). *Rev. Sci Inst*, (70) 180.
- [21] Hoskinson, A R. and Hershkowitz, R. (2006).*Plasma Sources Science Technology*, 15 (1) 85
- [22] Hendron, J. M. Mahony. C. M. O. Morrow, T and Graham, W. G.; (1997) *J. Appl. Phy*, **81**(5) 2131.
- [23] Huddlestone. R. H. (1965). *Plasma diagnostic Techniques*. Academic Press, New York and London.
- [24] Douglas, B. Chrisey. Graham, and Hubler, K. (1999). *Pulsed Laser Deposition of Thin Films*. John Willy & Sons Inc, New York.
- [25] Bhatti, K. A. Khaleeq-ur-Rahman, M. Rafique, M. S. Anwar, M.S. Perveen, N and Shahzad, M.:(2008) *Vacuum*, (82) 1157.
- [26] Khaleeq-ur-Rahman, M. Bhatti, K. A. and Rafique, M. S.. and Chaudhary ,K.T (2009).*Vacuum*,(83)936..